Full title

A heterotetrameric alpha-amylase inhibitor from emmer (*Triticum dicoccon* Schrank) seeds

Short title

Heterotetrameric alpha-amylase inhibitor

Authors names and affiliations

Capocchi A[1], Muccilli V[2], Cunsolo V[2], Saletti R[2], Foti S[2], Fontanini D[1]*

[1]Department of Biology, University of Pisa, Via L. Ghini 5, 56126 Pisa, Italy

[2]Department of Chemical Sciences, University of Catania, Viale A. Doria 6, 95125 Catania, Italy

Correspondence to: Fontanini Debora, Department of Biological Sciences, University of Pisa, Via L. Ghini 5, 56126, Pisa, Italy

Phone: +39 050 2211334

Fax: +39 050 2211309

E-mail: dfontanini@biologia.unipi.it

Abstract

Plants have developed a constitutive defence system against pest attacks, which involves the expression of a set of inhibitors acting on heterologous amylases of different origins. Investigating the soluble protein complement of the hulled wheat emmer we have isolated and characterized a heterotetrameric α-amylase inhibitor (ETI). Based on mass spectroscopy data, it is an assembly of proteins highly similar to the CM2/CM3/CM16 found in *durum* wheat. Our data indicate that these proteins can also inhibit exogenous α-amylases in binary assemblies. The calculated dissociation constants (K_i) for the pancreatic porcine amylase- and human salivary amylase-ETI complexes are similar to those found in *durum* and soft wheat. Homology modeling of the CM subunits indicate structural similarities with other proteins belonging to the cereal family of trypsin/α-amylase inhibitors; a possible homology modeled structure for a tetrameric assembly of the subunits is proposed.

Keywords

Triticum dicoccon, Heterotetrameric α-amylase inhibitor, CM protein, Tandem mass spectrometry, Kinetic study, Homology modeling

1. Introduction

Alpha-amylases (α-1,4-glucan-4-glucanohydrolases; EC 3.2.1.1) are hydrolytic enzymes widely distributed in nature (Franco, Rigden, Melo & Grossi-de-Sà, 2002), which catalyze the cleavage of the α-1,4 glycosidic linkages found in starch and other oligosaccharides. Cereal seeds stock large amounts of the substrate for these enzymes, making them vulnerable to the attack of pests and herbivores. Nonetheless, many plant species have developed a defence system against these attacks, which involve the expression of a set of seed inhibitors acting on a range of amylases of different origins. The plant proteinaceous inhibitors of α-amylases from humans and insects are collectively grouped into the structural family of the cereal trypsin/α-amylase inhibitors, which also comprises

proteins with the ability to inhibit trypsin-like proteinases (Salcedo et al., 2004). Many studies have been dedicated to these inhibitors and several of them have been isolated and characterized. Besides their defensive physiological role, the interest in these proteins lays in their possible use as potential source of genetic material for engineering pest-resistant crops (Franco et al., 2002) and their role in allergic diseases provoked by inhalation or ingestion of cereal flours (Salcedo et al., 2004). Wheat grains are particularly rich in inhibitors affecting heterologous amylases from insects and mammalians; despite the high identities between their sequences, some of these compounds inhibit specifically the insect α-amylases, while others are equally effective against the mammalian enzymes (Payan, 2004). The efficiency against the α-amylases from a particular source could be correlated with the inhibitors aggregation state (Silano, et al., 1975) and with particular traits and structural features of their protein sequences (Franco, Ridgen, Melo, Bloch, Silva & Grossi-de-Sà, 2000). The plant α-amylase inhibitors are highly diversified polypeptides encoded by disperse multi-gene families (García-Maroto, Marana, Mena, García-Olmedo & Carbonero, 1990), which act as monomers of about 12 kDa (Gomez, Sánchez-Monge, Lopez-Otin & Salcedo, 1991) homodimers of 24 kDa (Sánchez-Monge, Gomez, García-Olmedo & Salcedo, 1989) and heterotetramers of about 60 kDa (Gomez, Sánchez-Monge, García-Olmedo & Salcedo, 1989). The wheat tetrameric inhibitors are assemblies of three different subunits belonging to the class of the CM (chloroform/methanol-soluble) proteins, which typically result in 13-15 kDa polypeptides under dissociating conditions (Gomez et al.,1989). In the hexaploid wheat *Triticum aestivum* (AABBDD), five CM proteins (CM1, CM2, CM3, CM16 and CM17) have been identified (García-Olmedo, Salcedo, Sánchez-Monge, Rojo, & Carbonero, 1987) which aggregate with a complex pattern into heterologous α-amylases tetrameric inhibitor forms; however, a more distinct association has been described in *T. durum* (AABB), where the amylase tetrameric inhibitor has been described as an assembly of two CM3 subunits with one copy each of the CM2 and CM16 subunits (Gomez et al., 1989). Within our project of profiling the antinutritional and possibly allergenic proteins in seeds of the emmer tetraploid hulled wheat (*Triticum dicoccon* Schrank), we have been investigating its

76 soluble protein complement. During the isolation and characterization of two dimeric inhibitors of human salivary α-amylase (Fontanini et al., 2007a) we detected the presence of a component
78 showing similarities to the wheat tetrameric inhibitor described by Sánchez-Monge et al. (1982). The present work describes the isolation and characterization of this novel α-amylase inhibitor
80 which, based on mass spectroscopy data, was composed by an assembly highly similar to the CM2/CM3/CM16 found in common wheat. Our data indicate that these proteins can inhibit
82 exogenous α-amylases also in binary assemblies; this suggest that the potential range of action of these protein *in vivo* may be wider than originally conceived, indicating a possibly adaptative role.
84

2. Results

86 *2.1. Heterotetrameric inhibitor subunits purification*

The initial steps of the inhibitor subunits purification were based on detecting PPA, HSA and TMA
88 inhibition. *B. subtilis* and *H. vulgaris* α-amylases, were not affected by the emmer inhibitor (data not shown). As verified with SDS-PAGE, the separation by SEC gave inhibitory fractions
90 overlapping over a wide range of Mr; to fully resolve all of them, were needed three rounds of RP-HPLC and a considerable flattening of the gradient (down to 0.125% ACN/min). The last
92 fractionation gave four protein peaks (a, b, c, and h) eluting with 30.9%, 31.1%, 31.7% and 37.3% of solvent B, respectively (Fig. S1). MALDI TOF mass spectra of the isolated fractions showed the
94 presence of a main component at m/z 14156 in fraction a, a protein at m/z 13026 in fraction b, one with m/z 13428 in fraction c and a protein with m/z 15524 in fraction h (Fig. 1). The protein
96 fractions were analyzed by 2-DE which resolved them as single spots (Fig. 2A, peripheral boxes). Interestingly, fractions a and c had the same pI but different migration rates on gel. These samples
98 were further investigated by testing their glycosilation, using PAS staining on a 2-DE gel were a SEC partially purified inhibitor preparation was separated. A PAS-positive spot migrated
100 correspondingly with the protein purified as peak a, strongly indicating its glycosilation (Fig 2B). To investigate the identity of the protein fractions, the purified samples were first separated as

single spots by 2-DE; they were then excised, digested with trypsin and Glu-C, and analyzed by mass spectrometry. The results are summarized in Table I. All of the proteins isolated were identified as CM-proteins (see section *2.2*).

2.2. Subunits identification

Bioinformatic searches allowed the identification of the wheat proteins CM2, CM16 and CM3, with fractions b, c, and h, respectively (Acc. Nos. P16851, P16159, and P17314). Noticeably, fractions a and c were identified with the same subunit (CM16). In detail, the theoretical MH+ of 13022 Da for the emmer CM2 protein was coincident with the mass experimentally determined by MALDI mass spectrum. The analysis of the tryptic peptides of the protein excised from the 2D gel, confirmed 94% of the amino acid sequence, with the exception of peptides 47-48 (DR) and 62-66 (CEAVR) (Table I). However, based on the identity between the theoretical and experimental mass of the isolated subunit, the CM2 protein sequence could be considered as completely verified.

The analysis of the tryptic peptides of fraction h (Table I) allowed the identification of a CM3 subunit. The CM3 (143 aa), had a theoretical MH+ of 15823 Da. This mass value was 298 Da higher than the experimentally determined one at m/z 15525 Da. However, analyses of the tryptic peptides revealed the truncation of the last two amino acid of the sequence (WI) producing the C-terminal peptide YCPAVEQPL; this peptide sequence was manually verified by MSMS data interpretation. The analysis of the tryptic peptides covered the whole protein sequence except for the peptide CEALR (71-75). A parallel enzymatic digestion by Glu-C allowed coverage of the sequence 73-96, leaving unverified only the peptide CE (71-72). However, the theoretical MH+ of the C-terminus-truncated protein, was in agreement with the experimental mass detected by MALDI-MS. Therefore, the emmer protein sequence was identical to the wheat protein except for a deletion of the last two amino acids (WI) towards the carboxyl end.

The analysis of the peptides originated by the enzymatic cleavage of fraction c (Table I), allowed the identification of a CM16 protein. As for the CM2 subunit, the sequence could be considered 100% verified, since the theoretical MH+ of 13428 Da was in agreement with the experimental

128 value (m/z 13428). Nonetheless, neither the peptides obtained by trypsin cleavage nor those obtained by Glu-C cleavage of the protein could cover the peptide 57-61 (CQALR).

130 Finally, the analysis of the tryptic peptides from the peak a protein spot, identified this protein as a CM16 subunit. Interestingly, MALDI mass spectrum of the isolated subunit showed a complex

132 protein mixture with a main component at m/z 14156 which differs by 728 Da from the theoretical value of a the CM16 (MH^+ 13428 Da). Most of the amino acid sequence of this inhibitor was

134 verified, with the exception of the peptide sequence 57-61 and the C-terminal trait (fragment T9). The absence of the C-terminal peptide in the investigated m/z range, coupled with the evidence

136 from the PAS-stained gel for glycoprotein detection, strongly suggested that this peptide could carry a carbohydrate moiety at the unique N-glycosilation site (NLT; residues 100-102). Furthermore, the

138 mass difference of 728 between the theoretical and the experimental m/z value of the intact protein could suggest a linkage of $Man_2GlcNAc_2$-N-Asn.

140 *2.3. In vitro reconstitution experiments*

The single CM subunits and their binary and ternary mixtures were tested in inhibition assays

142 against HSA, PPA and TMA. To effectively test the α-amylase inhibition, it was measured over a range of assemblies concentration after having optimized the conditions for α-amylase activity. The

144 results confirmed what had already been observed; at all concentration tested, the single subunits were not able to inhibit any of the α-amylases, whereas the heterotetrameric assembly effectively

146 inhibited all of the amylase tested (Fig 3A). Nevertheless none of them was inhibited more than about 85% (data not shown).

148 When the purified subunits were mixed in all of the three possible binary combinations and tested for inhibition, each of the combinations studied gave comparable inhibition percentages against

150 HSA, PPA and TMA. The combination between CM2 and CM3 was the most effective in inhibiting all of the enzymes tested, reaching inhibition values very close to those found for the ternary

152 assembly. The combination CM3/CM16 was the second effective (about 50% final inhibition) while the assembly CM2/CM16 was the least effective, with final amylases inhibition of about 35% (Fig.

154 3B-D).

2.4. Reconstituted heterotetrameric inhibitor and binary mixture (CM2/CM3): kinetic inhibition

156 *studies of human saliva and hog pancreas α-amylases*

Using the kinetic procedure of Bieth (1974), K_i' (apparent K_i) values were graphically determined

158 for ETI (Fig. 4A) and the binary mixture (Fig. 4B) by equation (1). The heterotetrameric inhibitor K_i values obtained through (2), were 1.82 nM and 3.25 nM for PPA and HSA, respectively. Binary

160 mixture K_i values were 27 nM for PPA and 28.6 nM for HSA.

2.5. Homology modeling

162 The homology models for each of the CM inhibitory subunits, are shown in Figure 5A (sequence alignments in Fig. S2). The MODBASE server (Pieper et al., 2009) suggested the PDB entry 1b1uA

164 (*Eleusine coracana* bifunctional trypsin/α-amylase inhibitor) as the most likely template for building the CM2 and CM16 subunits homology models (45% and 41% identity with the sequence

166 template, respectively), and 1bea (Hagemann factor from maize; 50% identity) as template for the CM3 model. These values of sequence identity between the emmer CM proteins and the selected

168 templates well satisfied the similarity criteria based on which homology models can be expected to be successfully created (Chothia & Lesk, 1986). Homology models for each of the subunits were

170 built by using the GUI Easy Modeller 2.0 for MODELLER. Although the emmer CM proteins showed a certain degree of sequence similarities (45-48 %) and conservation, the CM3 had non-

172 aligned residue stretches which formed extra or longer loops (Cys 27-Pro 34; Met 40-Lys 50; Ser 84-Asp 88). In spite of the loop modeling and optimization functions implemented in the GUI, a

174 CM3 subunit model relaxed from a knot in a protein long loop (27-51), was obtained only after submitting the sequence to the ModBase server for automatic modeling. The CM models obtained

176 had estimated RMSD within 2.1 and 2.2 and DOPE energies between -0.7 and -1.5. Overall, between 82 and 85% of the residues were found in the most favoured regions of the Ramachandran

178 plot, with 1 (CM2 model) or 2 (CM3 and CM16 models) residues in the disallowed regions.

To build a possible tetrameric structure for the hypotetical $CM2(CM3)_2CM16$ emmer aggregate, the

PISA sever at the EBI was interrogated to search for the most likely polymeric aggregation state for the CM model templates. The template 1bea was recognized as the only likely to form a tetrameric aggregate in solution. The structure of the homotetramer $(1bea)_4$ was then used as template to build a possible theoretical quaternary structure for the emmer inhibitor. The homology modeling interface EasyModeller was used to design six alternate models having as sequences the six possible quaternary aggregations of the three CM subunits. It is to notice that to this end, the CM2 and CM16 subunits had to be modeled onto the template 1bea instead of the more favourable 1b1ua. The Modeller/EasyModeller energy evaluation tools (the set of statistical potentials GA341, DOPE, CαRMSD and the native overlap value, NO3.5), basing the evaluation on comparative rather than absolute values, are well suited to assess the reliability of alternative models. Based on these values, the best-scoring heterotetrameric model was the one built on the lined-up sequence CM3:CM2:CM3:CM16. However, when the six models were subjected individually to validation with PROCHECK (Laskowski, MacArthur, Moss & Thornton, 1993) and structural assessment with the appropriate Swiss-Model tool (Peitsch, 1995; Kiefer, Arnold, Kunzli, Bordoli & Schwede, 2009), the model scoring third based on DOPE energy (CM2:CM3:CM3:CM16), had the overall best value. In fact, 76.5% of itsresidues were in the most favourable region of the Ramachandran plot, 18.6% in the allowed, 3.1% in the generously allowed region and 1.7% was found in the disallowed region (7 residues; Leu 200, Thr 288, Phe 289, Leu 339, Gln 344, Asp 399, Trp 403). This was also the only model having an overall average G-factor at the edge of the range of "usual" values (-0,51). Hence, the model corresponding to the sequence CM2:CM3:CM3:CM16 was selected as the ETI model (Fig. 5B).

2.6. Modeling of ETI interaction with the TMA reactive site

The interaction between the inhibitor and the TMA reactive site, was modeled based on the crystal structure of the ragi (*E: coracana)* trypsin/α-amylase inhibitor in complex with the *T. molitor* α-amylase (1TMQ). To this end, the ETI model was docked onto the TMA structure extracted from 1TMQ. Among the 10 models returned by the docking server, three were selected for having an

206 orientation similar to that adopted by RBI in its complex with TMA, relatively to the enzyme active site. Of these, one was selected as most fitting on the basis of its estimated contacts with the TMA
208 active site (Fig. 5C and Fig. S3); the theoretical hydrogen bonds and favourable direct interactions (polar and non polar) forming between the modeled inhibitor and the TMA structure in this docking
210 scenario, are shown in Table SI. These interactions comprise 22 inhibitor aa and 32 TMA aa, including those involved in possible hydrogen bonds, among which are the enzyme's catalytic
212 residues; in particular, an hydrogen bond is supposedly formed between the inhibitor Ser 164 and the TMA Glu 222.

214

3. Discussion

216 Plant proteinaceous tetrameric inhibitors identified in cereal seeds (Buonocore, De Biasi, Giardina, Poerio, & Silano, 1985; Sánchez-Monge, Gomez, García-Olmedo, & Salcedo, 1986) act against
218 heterologous α-amylases with different specificities. Here, we have isolated a heterotetrameric inhibitor (ETI) from emmer seed flour, active against HSA, PPA and TMA. The *H. vulgaris* α-
220 amylase was not sensitive to the emmer inhibitor, confirming the specificity of the members of the cereal α-amylase/trypsin inhibitor family for heterologous enzymes (Salcedo et al., 2004). Although
222 our purification process was designed for selecting the higher Mr inhibitory fractions, the tetrameric protein conformation was lost during the purification process due to quaternary structure instability
224 to the RP-HPLC conditions. Although the polymeric nature of the emmer protein could not be demonstrated from the beginning, during the protein purification became clear that its inhibitory
226 capacity was weakened or lost when particular HPLC fractions were taken apart; however it was recovered during the assays when those, which later were identified as inhibitor protomers, were
228 allowed to re-assemble into an active form. By the end of the purification process, four pure subunits (a, b, c, and h) were obtained with apparent Mrs of about 14-15 kDa. Two-dimensional
230 electrophoresis of fraction a indicated its glycosilation and that its pI, but not the migration rate, was equal to that of fraction c. These data, coupled with the MS spectra of the intact protein and

232 sequence verification, suggested that the protein corresponding to fraction a, may be a glycosilated form of the fraction c protein. The mass difference of about 728 Da between the fraction a and c
234 detected by the MALDI mass spectra, was compatible with different combinations of sugar residues and lied within the range of known plant N-linked glycopeptides. A similar mass difference was
236 determined based on MS data for a possibly glycosilated rye α-amylases inhibitor (Iulek et al, 2000). Sanchez-Monge et al. (1992) have shown the glycosilation of the *durum* wheat CM16
238 protein (CM16*) and its barley counterpart Cmb. Interestingly, the authors have also found that these proteins are about ten-fold less abundant than their non-glycosilated forms, as was the emmer
240 fraction a as compared with fraction c (data not shown). Future attempts will be made to investigate the complex carbohydrate moiety by MS approaches.
242 Fractions b, c and h were identified with CM-proteins by MS analyses. The emmer CM-proteins were identical to the tetraploid common wheat CM subunits CM2, CM3, CM16, which aggregate *in*
244 *vivo*, in a heterotetrameric α-amylase inhibitor (Gomez et al., 1989) and have close relatives in the analogous subunits of the barley heterotetrameric inhibitor (Cma, Cmd, Cmb, respectively). It was
246 found that the wheat and barley subunits were active against TMA and HSA only when three of them aggregated in the inhibitory tetramer. However, the emmer CM subunits were also active in
248 binary combinations against all of the three α-amylase tested, a data which is in contrast with the findings of Gomez et al. (1989). The presence of the CM3 subunit in the most active binary
250 combinations suggested an important role for this protomer in strengthening the α-amylase activity inhibition.
252 The emmer inhibitor never reached 100% of inhibition in the HSA-, TMA- and PPA-inhibition assays. Lack of complete α-amylase inhibition is a common feature of the protein inhibitors, which
254 never totally block their target enzyme activity. An explanation for this behaviour was given for the ragi α-amylase/trypsin bifunctional inhibitor (RATI). RATI inhibition kinetics did not obey a
256 simple mechanism of competitive inhibition due to binding of the inhibitor to the amylase starch substrate (Alam, Gourinath, Dey, Srinivasan & Singh, 2001). Buonocore et al. (1985) showed that

the starch hydrolysis by the *T. molitor* amylase in the presence of the wheat heterotetrameric inhibitor, became linear only after a short lag period, during which the complex α-amylase:inhibitor partly dissociated upon starch addition to the reaction mixture. Those data convey that complete inhibition of the amylase activity cannot be achieved due to substrate competition with the inhibitor for binding the α-amylase. The emmer α-amylase-inhibition kinetics has been studied by applying the approach designed by Bieth (1974), for that protein-protein interaction characterized by tight-binding. In that case, the proportion of inhibitor involved in the complex with the enzyme is not negligible and classical equations cannot be used for the graphical determination of K_i. Goldstein (1944), showed that when the *E*t/*K*i ratio is comprised between 0.01 and 100, the inhibitor concentration is significantly reduced by its interaction with the enzyme, and the conditions for tight-binding inhibition are attained. Although the inhibitor binds the enzymes very strongly, the introduction of the substrate into an equilibrium enzyme-inhibitor mixture may cause the complex dissociation; here, the binding behaviour will be substrate-dependent. The E_t/K_i ratios obtained by our experimental data were within the range supporting tight-binding inhibition (data not shown). The K_i values estimated with Bieth's equations were very close to those obtained for the systems TMA-tetrameric inhibitor (Buonocore et al., 1985), TMA- wheat inhibitor 0.19 and TMA- wheat inhibitor 0.28 (Buonocore, Gramenzi, Pace, Petrucci, Poerio & Silano, 1980). The kinetic treatment of the inhibition assay data for the CM2/CM3 binary mixture gave K_i values which confirmed the lower affinity towards HSA and PPA of the CM2/CM3 binary mixture as compared to the heterotetrameric assembly. To the best of our knowledge, this is the first report on the kinetics of α-amylases inhibition by a reconstituted cereal seed heterotetrameric inhibitor.

To understand the possible role of the CM subunits in the amylase inhibition, we attempted to build a structural model of the complex between ETI and one of the amylases against which is active. Since no 3-D model was available for any of the wheat CM subunits purified, nor for the tetrameric inhibitor protein, the single subunit 3-D homology models were built first. These models were based on the tertiary structure of the ragi α-amylase inhibitor (CM2 and CM16) and the Hagemann

284 factor from maize (CM3), which scored the highest identities with the target proteins. The CMs 3-D structures, built around four α-helices arranged in an “up and down” pattern, resembled closely that
286 of RBI; they were also topologically similar to other members of the cereal trypsin/α-amylase inhibitor family, the wheat 0.19 dimeric and the 0.28 monomeric inhibitors of α-amylase (Oda,
288 Matsunaga, Fukuyama, Miyazaki, & Morimoto, 1997; Payan, 2004), despite the little sequence identities (17-23 % with 0.19 and 17-19% with 0.28).
290 The CM subunits were modeled into a heterotetramer in which the CM3 was present in two copies as suggested by Gomez et al. (1989) When interrogated for the interaction between the TMA
292 structure and ETI model, the automatic docking server GRAMM-X returned a structure which fitted the inhibitor into the α-amylase active site groove. This model well agreed with the RBI:TMA
294 complex, as its crystallography data showed the inhibitor sitting in a V-shaped depression comprising the TMA active site (Strobl, Maskos, Wiegand, Hubert, Gomis-Ruth, & Glockshuber,
296 2004) and centered around the residues Asp 185, Glu 222 and Asp 287. Moreover, RBI was bound to the active site and interacted with residues of the TMA domains A and B flanking the active site.
298 In the complex, the α-amylase subsites were completely blocked by the inhibitor; essential were the N-terminus residues Ser 1-Ala 11 and Pro 52-Pro 55, which penetrated the substrate binding groove
300 and directly targeted the catalytic residues (Payan, 2004). The binding with Asp 287 was also sufficient to block the TMA activity in the case of the amaranth α-amylase inhibitor AAI (Barbosa
302 Pereira et al., 1999). In the *Phaseolus vulgaris* α-AI1 complexed with PPA, HSA and TMA (Bompard-Gilles, Rosseau, Rouge, & Payan, 1996 Nahoum et al., 1999; 2000), the inhibitor was
304 also bound to the enzymes active site, and its strong contacts with the enzymes catalytic groove were highly conserved (Payan, 2004). In the modeled interaction between the ETI and TMA, the
306 first CM3 subunit along the primary structure sat in the TMA active site depression. As already discussed, parts of this subunit sequence were modeled into long loops which protrude off the
308 protein main body. Consequently, the modeled interaction between TMA and ETI, contemplated an hairpin loop penetrating the enzyme catalytic cleft, in a similar manner as the complex between the

bean α-AI1 and its target enzymes. However, this kind of interaction was quite different from that found in 1TMQ, where the N-terminal segment curls into the TMA depression (Payan, 2004), rather than the long loop joining helices α1 and α2 of the first CM3. The number and location of the estimated contacts between these two proteins, involving all the catalytic residues, would explain the inhibitory effect of the tetrameric protein. The residues contacting the TMA active site region were located within the sequences Phe 150-Lys 175 and Lys 236-Gln 242 of the first CM3 in the tetramer primary structure, and Pro 428-Gly 429 of the CM16; of these, 90.5% belonged to the CM3 subunit. This extended interaction of the CM3 subunit would explain the significant TMA inhibition carried out by its binary combination with another CM protein; in the present model, the CM2 subunit had no contacts with the enzyme. However, the CM2 subunit and the second CM3 (along the primary structure) made up the bulk of the inhibitor side opposite to the TMA binding-region. The large size of the heterotetrameric molecule, compared with the CM2/CM3 assembly, could determine a more efficient steric hindrance for the starch substrate to reach the TMA; on the other hand, it would increase its ability to contrast the mutual depletion exerted by the starch substrate. Overall, independently by the identity of the combined subunits, we have found that whenever more than one of the CM subunits aggregate, the resulting molecule is able to exert a certain degree of inhibition. The flexibility in the re-assembly of α-amylase inhibitor subunits, has also been shown by Zoccatelli et al. (2007) for the dimeric inhibitors from *durum* and soft wheat, suggesting that the expression of several different proteins able to exert their inhibitory function against heterologous α-amylases, even in different combinations, could be a general strategy adopted by cereal seeds to better respond to predator attacks.

4. Concluding Remarks

Like common wheat, emmer expresses in its seeds an inhibitor of α-amylases. This protein is a heterotetrameric assembly of CM subunits highly identical to their homologous found in *durum* wheat. Interestingly, these emmer subunits can inhibit the same amylase activities also in binary

assemblies, whereas the *T. durum* subunits were inhibitory only in the heterotetrameric aggregate. The structural model proposed for the emmer α-amylase inhibitor hints to possible role of the subunits in the inhibition mechanism carried out by the heterotetrameric and binary assemblies of these protein inhibitors.

5. Experimental

5.1. Material

Emmer seeds were purchased from the Consorzio Produttori Farro della Garfagnana (Piazza al Serchio, Lucca, Italy). The seeds were ground for 2 min and 30 sec in a steel balls mill (Retsch GmbH & Co. KG, Haan, Germany) cooled with dry ice. The flour was used immediately.

5.2. Purification of the α-amylase inhibitor subunits.

Fifty grams of emmer flour were extracted twice by continuous stirring with 250 ml of 0.15 M NaCl for 1 hour. After centrifuging the slurry at 15,000 rpm for 15 min, the supernatant was brought to 50% saturation with solid ammonium sulphate and stirred for 30 min. After centrifugation (15,000 rpm for 15 min), the precipitate was suspended in 20 mM sodium acetate buffer, pH 5.3, and dialyzed overnight (3.5 kDa MWCO) against 4 L of the same buffer. The extract was centrifuged as above and the supernatant was chromatographed on a CM column (2.5 x 15.5 cm; Sigma-Aldrich, Milan, Italy) equilibrated with 20 mM sodium acetate buffer, pH 5.3 . After washing with 100 mM sodium acetate buffer, the column was eluted with a gradient of the sodium acetate buffer (100-300 mM in 200 ml). The eluted fractions were assayed for HSA inhibitory activity after adjusting their pH to 6.9 with 0.4 M Na_2HPO_4. Three inhibitory pools were recovered; the one eluted with the 100 mM buffer-wash was subjected to further purification by SEC. All the above procedures were carried out at 4 °C.The lyophilized CM-pool was dissolved in 20 mM sodium phosphate buffer, pH 7.0, containing 0.13 M NaCl and injected on a Zorbax GF-250 column (9.4 mm x 250 mm, 150 Å, 4 μm; Agilent, Milan, Italy) for SEC. The fraction of interest was collected, dialyzed extensively against 5 mM ammonium acetate, pH 6.9, and freeze-dried. The lyophilized sample was dissolved

362 in 80% solvent A (H_2O-0.05% TFA) and 20% solvent B (CH_3CN-0.05% TFA), and injected on a semi-preparative C18 RP-HPLC column (Nucleosil, 10 mm x 250 mm, 300 Å, 7 µm; Macherey-
364 Nagel GmbH & Co. KG, Düren, Germany). The separation was achieved at 50 °C with a two-steps linear gradient going from 20% to 30% of solvent B in 10 min, and from 30% to 50% of solvent B
366 in 80 min, at a flow rate of 3 ml/min. Final protein purification was achieved by chromatography of the lyophilized fractions onto an analytical C18 column (Nucleosil, 4 mm x 250 mm, 300 Å, 5 µm;
368 Macherey-Nagel GmbH & Co. KG, Düren, Germany) equilibrated with 80% solvent A and 20% solvent B.

370 The elution was performed at a flow rate of 1 ml/min, with a two-steps linear gradient going from 20% to 30% solvent B in 10 min, and from 30% to 50% solvent B in 60 min, at 50 °C. The
372 collected peaks were re-chromatographed on the same analytical column with a solvent B gradient that went from 20% to 30% in 10 min and from 30% to 50% in 160 minutes. Protein fractions were
374 analyzed for purity by 15% SDS-PAGE (Laemmli, 1970) and quantitated with the Bradford method (Bradford, 1976).

376 *5.3. MALDI-TOF MS of isolated subunits.* The MALDI mass spectrum of the isolated inhibitors, acquired in the mass range 10000-20000 Da, was obtained as described in Fontanini et al. (2007a)
378 The accuracy of the molecular masses determination by MALDI-TOF was 0.04%.*5.4. In-gel digestion of protein spots and mass spectrometric analyses.* Selected protein spots from the 2-DE
380 gel were excised, washed and subjected to in-gel trypsin or endoproteinase Glu-C digestion (Shevchenko, Wilm, Vorm & Mann,1996). After soaking trypsin (Modified porcine trypsin,
382 Promega, Madison, WI) or endoproteinase Glu-C (Sigma-Aldrich, Milan, Italy) into the gel pieces, the supernatant was removed and the gel pieces were covered with 50 µl of 50 mM NH_4HCO_3 and
384 incubated at 37 °C overnight. The reaction was stopped by cooling the gel pieces and the supernatant soln. at -24 °C. MALDI-MS analyses of the peptides were performed as described in
386 Fontanini et al.(2007a). The m/z software (Proteometrics Ltd, New York, NY, USA) was used to analyze the MALDI-TOF spectra.

388 *5.5. Bioinformatic search.* MALDI-TOF peptide mass data were used to perform protein identifications by searching the NCBInr database using an in-house Mascot server *2.3* in the PMF
390 mode. The following parameters were used for database searches: taxonomy, *viridiplantae* (green plants); mono-isotopic mass accuracy, 100 ppm; missed cleavages, 2; allowed modifications,
392 propionamide Cys (fixed), oxidation of Met (variable), transformation of N-terminal Gln and N-terminal Glu residue in the pyroglutamic acid form (variable).

394 *5.6. Capillary RP-HPLC/nESI-MSMS.* Capillary RP-HPLC/nESI-MSMS was performed using a Ultimate 3000 system (LC Packings, Dionex, Sunnyvale, CA, USA) coupled with a linear ion trap
396 nano-electrospray mass spectrometer (LTQ, Thermo Electron, San Jose, CA). After in-gel digestion, the digested soln. was transferred into a clean 0.5-ml tube. The peptides were extracted
398 from gel pieces with 40 µl of 5% FA and subsequently with an equal volume of CH_3CN. This extraction procedure was repeated three times. The total extracts were pooled, lyophilized and re-
400 dissolved in 20 µl of 0.5% FA. Ten µl of the peptide solution was directly loaded onto a C18 µ-pre-column (30 x 5 mm, 100 Å, 5µm, PepMap, LC Packings, Dionex, Milan, Italy) with 0.5% aqueous
402 FA at a flow rate of 20 µl/min for 4 min. The peptides were then applied onto a C18 capillary column (150 x 0.18 mm, 300 Å, 5µm, Thermo Electron, Milan Italy) and eluted at room temp. with
404 a linear gradient of CH_3CN-0.5% FA/H_2O-0.5% FA from 5 to 50% in 50 min at a flow rate of 2 µl /min. The nESI source operated under the following conditions: source temp. 220 °C, source
406 voltage 1.9 kV and capillary voltage 42 V. Repetitive mass spectra were acquired in positive ion mode in the m/z range 350–2000. Characterization of peptide ions was performed by the data-
408 dependent method as follows: (1) full scan MS in the m/z range 350–2000; (2) zoom scan of the five most intense ions (isolation width: 2); (3) MS/MS analysis of the five most intense ions
410 (normalized collision energy: 24 a.u., activation *Q*: 0.250, isolation width 2 Da). Mass calibration was made using a standard mixture of caffeine (Mr 194.1 Da), MRFA peptide (Mr 523.6 Da) and
412 Ultramark (Mr 1621 Da). Data analysis and sequence data handling were performed using the General Protein/Mass Analysis for Windows (GPMAW) software.

5.7. Tenebrio molitor α-amylase extraction. Tenebrio molitor larvae were kindly provided by Microvita (Crespellano Bologna, BO, Italy). The liophilized larvae (5 g) were homogenized with Polytron (Kinematica, Inc., Bohemia, NY) homogenizer on ice, in 10 volumes of 20 mM sodium phosphate buffer, pH 5.4, containing 6.7 mM NaCl. The homogenate was stirred for 1 hr at 5 °C. The extract was centrifuged at 15,000 rpm for 10 min, at 4 °C and the supernatant was used as source of amylase activity. The amount of TMA used in the inhibition assays was chosen in the range of that gave linear activity response under the assay conditions (data not shown).

5.8. Alpha-amylase activity and inhibition assay. The activity of the α-amylases from human saliva (HSA), *Bacillus subtilis* (type II-A), barley (*Hordeum vulgare*) malt (type VIII-A), and hog pancreas (PPA) (all from Sigma-Aldrich, MI, Italy) were measured according to our modification of the Bernfeld assay (Fontanini, Capocchi, Saviozzi & Galleschi, 2007b). The assays were carried out in 20 mM sodium phosphate, pH 6.9, buffer containing 6.7 mM NaCl; TMA activity was assayed at pH 5.4. The inhibition assays were performed by adding appropriate amounts of inhibitor preparation in the pre-incubation mixture. The inhibitor samples were always treated for 5 min at 100 °C before being added to the assay mixture. Control assays were run as described in Fontanini et al.(2007a) All assays were performed in triplicate unless specified otherwise.

When testing inhibition of the purified subunits and their *in-vitro* assemblies (binary and ternary mixtures), proteins were dissolved in water and the assays performed with five replicates.

5.9. Kinetic inhibition study of HSA and PPA by the heterotetrameric inhibitor and by a binary mixture of the CM2 and CM3 subunits. The activities of HSA and PPA were measured as described above, against five soluble starch concentrations (2-10 mg/ml). Kinetic parameters were obtained by linear regression of the Hanes–Woolf representation of the Michaelis-Menten equation. All assays were ran with five replicates.

Kinetic inhibition studies were performed with the emmer tetrameric inhibitor (ETI) reconstituted (CM2/CM3/CM16), and with the binary mixture formed by the CM2 and CM3 subunits. For the

HSA-inhibition assays, ETI concentration ranged from 18 to 54 nM, while in the PPA-inhibition assay was from 9 to 45 nM; the binary mixture CM2/CM3 used in the HSA-inhibition assay was 64.28-167.14 nM and 45-141.43 nM in the PPA-inhibition assay. All assays were ran in five replicates and were performed as described above.

The equations:

$$[I_0] / 1 - a = 1/a \cdot K_i' + [E_0] \quad (1)$$

$$K_i' = K_i \cdot (1 + [S_0] / K_m) \quad (2)$$

(where $a = V_i/V_0$) were used to calculate the amylase-inhibition kinetic parameters by applying an approach designed for mutual depletion systems (Bieth, 1974), characterized by a tightly bound enzyme-inhibitor complex which partially dissociates upon substrate addition.

5.10. 2-DE of the α-amylase inhibitor subunits. Ten micrograms of each isolated inhibitory fraction were added with 25 mM Tris-HCl, pH 9.0, containing 2% CHAPS, 7 M urea, 2 M thiourea, 0.5% IPG buffer (pH 3-10) and traces of BPB. The sample was reduced with 43 mM DTT for two hours, alkylated for one hour with 60 mM acrylamide and applied on an Immobiline DryStrip gel (7 cm, pH 3-10; Amersham Biosciences, Milan, Italy) by overnight rehydration. Isoelectric focusing was performed at 20 °C with a Multiphor II apparatus (Amersham Biosciences, Milan, Italy) for 1 min at 200 V, followed by a linear voltage gradient up to 3,500 V in 90 min, and 1 hour of constant voltage (3,500 V). The strip was then equilibrated in 50 mM Tris-HCl, pH 8.8, containing 6 M urea, 30% glycerol, 2% SDS and traces of BPB (equilibration buffer) added with 25 mM DTT. After 20 min, the strip was put in alkylating equilibration buffer containing 360 mM acrylamide for 20 min more. The second dimension separation was performed on a 15% SDS-PAGE minislab gel. The minigel was stained with 0.02% PhastGel Blue R-350 and destained with methanol:acetic acid:water (3:1:6, v:v:v).

5.11. PAS glycoprotein staining. SDS-PAGE gels were stained for glycoproteins with fuchsine after fixing with 12.5% TCA (Zacharius, Zell, Morrison & Woodlock, 1969). For positive control, 2 µg

464 each of hemocyanin from keyhole limpet and horseradish peroxidase (both from Sigma, Saint Louis, MO, USA) glycoprotein standards were also applied on the gel.

466 *5.12. Homology modeling.* Multiple sequences alignments were carried out with ClustalW2 (Larkin et al., 2007) and Bioedit sequence alignment editor (Hall, 1999).

468 The CM subunits model were built based on templates retrieved from MODBASE (Pieper et al., 2009) by submitting the accession numbers P16851 (CM2), P17314 (CM3), and P16159 (CM16),

470 as identified by the MS analyses of the purified subunits.

The homotetrameric inhibitor model template (A_4) was retrieved from the Protein interfaces,

472 surfaces and assemblies service, PISA, at the European Bioinformatics Institute (http://www.ebi.ac.uk/msd-srv/prot_int/pistart.html) (Krissinel & Henrick, 2007), by interrogating the

474 server for likely assemblies of the 1bea structure, using the default parameters.

Homology models for each of the CM inhibitory subunits identified by MS/MS and ETI, were built

476 either using Modeller (Šali & Blundell 1993) at the ModWeb server, or the GUI EasyModeller 2.0 for Modeller (Kuntal, Aparoy & Reddanna, 2010), with the default parameters.

478 Six heterotetrameric models of all the possible 4-ways combinations of the three CM subunits were built based on the formula $CM2(CM3)_2CM16$. The crystallographic data of the A_4 assembly from

480 the PISA server served as template, while the query sequence was a Fasta file of the CM sequences lined-up as needed. The best alignment between the query sequences and the template sequence was

482 selected by the software and visually inspected by using the Bioedit sequence alignement editor implemented into EasyModeller. Models graphical visualitazion was performed with the UCSF

484 Chimera package (http://www.cgl.ucsf.edu/chimera) (Pettersen et al., 2004).

For analyzing the interaction between the ETI homology model and the TMA active site, the

486 inhibitor model was docked onto the TMA structure extracted from 1TMQ (http://dx.doi.org/10.2210/pdb1tmq/pdb), the crystal structure of RBI complexed with TMA. The

488 docking simulation was performed by using the GRAMM-X protein docking server (http://vakser.bioinformatics.ku.edu/resources/gramm/grammx) (Tovchigrechko & Vakser, 2006) which

490 output was a set of alternative .pdb files. Clash and contacts, as well as the Hbonds formation between the inhibitor model and the TMA active site, were calculated by using the Chimera
492 software corresponding tools.

494 **Figure Legends**

Figure 1. MALDI-TOF mass spectra of the RP-HPLC fraction a, b, c and h, acquired in the 10000-
496 2000 m/z range.

Figure 2. Two-dimensional electrophoresis of the purified inhibitory fractions. A. The samples a-h
498 were separated by 2-DE (IEF X PAGE; pI range 3-10, 15% acrylamide). The central box represents a composite image obtained by superimposing the peripheral gels. B. 2-DE (IEF X PAGE; pI range
500 3-10, 15% acrylamide) of a partially purified emmer flour extract. Upper box, gel stained for proteins with CBB-R; lower box, gel PAS-stained for glycoproteins detection. The insert replicates
502 the gel labelled as "peak a" from figure 2A. The arrows indicates the same spot on each gel, as matched after accurate superimposition of the gel images. All of the gels were cropped to show only
504 areas of interest.

Figure 3. Inhibitory activity against the a-amylases from human saliva (HSA), hog pancreas (PPA),
506 and *Tenebrio molitor* larvae (TMA). A, inhibition by the heterotetrameric inhibitor reconsituted from the purified CM subunits (CM2, CM3 and CM16). B-D, inhibition by binary assemblies of the
508 purified CM subunits. Within each graph are indicated the binary mixtures used as inhibitor source.

Figure 4. Kinetic treatment of HSA- and PPA-inhibitor complexes, as mutual depletion systems. A.
510 Heterotetrameric inhibitor (HSA: 18 nM, 27 nM, 36 nM, 45 nM, 54 nM; PPA: 9 nM, 18 nM, 27 nM, 36 nM, 45 nM). B. Binary subunits assembly (HSA: 64.3 nM, 90 nM, 115.7 nM, 141.4 nM,
512 167.1 nM; PPA: 45 nM, 64.3 nM, 90 nM, 115.7 nM, 141.4 nM). The plots allow calculation of apparent dissociation constants according to equation (1).

514 **Figure 5.** ETI and CM subunits modeling. A, homology models of the CM2, CM3 and CM16 subunits. B, homology model of the heterotetrameric inhibitor built on a $(1bea)_4$ template (PDB

entry 1bea, Hagemann factor from maize). C, structural model of the interaction between TMA (surface model, green) and ETI (ribbon model, orange). TMA aminoacids involved in contacts with the inhibitor are in light green; inhibitor amino acids involved in contacts with TMA are in yellow. The TMA catalytic site amino acids are depicted in blue whereas the inhibitor amino acids involved in contacts with the enzyme active site are depicted in red.

References

Alam, N., Gourinath, S., Dey, S., Srinivasan, A., & Singh, T.P., 2001. Substrate-inhibitor interactions in the kinetics of α-amylase inhibition by ragi α-amylase/trypsin inhibitor (RATI) and its various N-terminal fragments. Biochemistry 40, 4229-4233.

Barbosa Pereira, P.J., Lozanov, V., Patthy, A., Huber, R., Bode W., Pongor, S., Strobl, S., 1999. Specific inhibition of insect α-amylases: yellow meal worm α-amylase in complex with the *Amaranth* alpha-amylase inhibitor at 2.0 Å resolution. Structure 7, 1079-1088.

Bieth, J. (1974) Some kinetic consequences of the tight binding of protein-proteinase-inhibitors to proteolytic enzymes and their application to the determination of dissociation constants. Bayer-Symposium V “Proteinase Inhibitors”, pp.463-469.

Bompard-Gilles, C., Rosseau, P., Rouge, P., Payan, F., 1996. Substrate mimicry in the active center of the mammalian α-amylase: structural analysis of an enzyme-inhibitor complex. Structure 4, 1441-1452.

Bradford, M., 1976. A rapid and sensitive method for the quantitation of microgram quantities of protein utilizing the principle of protein-dye binding. Anal. Biochem. 72, 248–254.

Buonocore, V., De Biasi, M.G., Giardina, P., Poerio, E., Silano, V., 1985. Purification and properties of an α-amylase tetrameric inhibitor from wheat kernel. BBA 831, 40-48.

Buonocore, V., Gramenzi, F., Pace, W., Petrucci, T., Poerio, E., Silano, V., 1980. Interaction of wheat monomeric and dimeric protein inhibitors with α-amylase from yellow mealworm (*Tenebrio molitor* L: larva). Biochem. J. 187, 637-645.

542 Chothia, C., Lesk, A.M., 1986. The relation between the divergence of sequence and structure in proteins. EMBO J. 5, 823–826.

544 Fontanini, D., Capocchi, A., Muccilli, V., Saviozzi, F., Cunsolo, V., Saletti, R., Foti, S., Galleschi L., 2007a. Dimeric inhibitors of human salivary α-amylase from emmer (*Triticum dicoccon*

546 Schrank) seeds. JAFC 55, 10452-10460.

Fontanini, D., Capocchi, A., Saviozzi, F., Galleschi, L., 2007b. Simplified electrophoretic assay for

548 human salivary α -amylase inhibitor detection in cereal seed flours. JAFC 55, 4334-4339.

Franco, O.L., Rigden, D.J., Melo, F.R., Grossi-de-Sá, M.F., 2002. Plant α-amylase inhibitors and

550 their interaction with insect α-amylases. Structure, function and potential for crop protection. Eur. J. Biochem. 269, 397-412.

552 Franco, O.L., Rigden, D.J., Melo, F.R., Bloch, C.Jr., Silva, C.P., Grossi-de-Sá, M.F., 2000. Activity of wheat α-amylase inhibitors towards bruchid α-amylases and structural explanation of observed

554 specificities. Eur. J. Biochem. 267, 2166-2173.

García-Maroto, F., Marana, C., Mena, M., García-Olmedo, F., Carbonero, P., 1990. Cloning of

556 cDNA and chromosomal location of genes encoding the three types of subunits of the wheat tetrameric inhibitor of insect α-amylases. Plant. Mol. Biol. 14, 845-853.

558 García-Olmedo, F., Salcedo, G., Sánchez-Monge, R., Gomez, L., Rojo, J., Carbonero, P., 1987. Plant proteinaceous inhibitors of proteinases and α-amylases. Oxf. Surv. Plant Mol. Cell. Biol. 4,

560 275-334.

Goldstein, A., 1944. The mechanism of enzyme-inhibitor-substrate reactions. J. Gen. Physiol. 27,

562 529-580.

Gomez, L., Sánchez-Monge, R., García-Olmedo, F., Salcedo, G., 1989. Wheat tetrameric inhibitors

564 of insect α-amylases: alloploid heterosis at the molecular level. PNAS 86, 3242-3246.

Gomez, L., Sánchez-Monge R., Lopez-Otin, C., Salcedo, G., 1991. Wheat inhibitors of

566 heterologous α-amylases. Characterization of major components from the monomeric class. Plant Physiol. 96, 768-774.

568 Hall, T.A., 1999. BioEdit: a user-friendly biological sequence alignment editor and analysis program for Windows 95/98/NT. Nucleic Acids Symp. Ser. 4, 95-98.

570 Iulek, J., Franco, O.L., Silva, M., Slivinski, C.T., Bloch, C.Jr., Rigden, D.J., Grossi-de-Sá, M.F., 2000. Purification, biochemical characterization and partial primary structure of a new α-amylase

572 inhibitor from *Secale cereale* (rye). Int. J. Biochem. Cell. Biol. 32, 1195-1204.

Kiefer, F., Arnold, K., Künzli, M., Bordoli, L., Schwede, T., 2009. The SWISS-MODEL

574 Repository and associated resources. Nucleic Acids Res. 37, D387-D392.

Krissinel, E., Henrick, K., 2007. Inference of macromolecular assemblies from crystalline state. J

576 Mol Biol, 372, 774-797, PDBePISA, (http://www.ebi.ac.uk/msd-srv/prot_int/pistart.html).

Kuntal, B.H., Aparoy, P., Reddanna, P., 2010. EasyModeller: A graphical interface to

578 MODELLER. BMC Res. Notes 3, 226-230.

Laemmli, U.K., 1970. Cleavage of structural proteins during the assembly of the head of

580 bacteriophage T4. Nature 227, 680-685.

Larkin, M.A., Blackshields, G., Brown Chenna, N.P.R., McGettigan, P.A. McWilliam, H.,

582 Valentin, F., Wallace, I.M., Wilm, A., Lopez, R., Thompson, J.D., Gibson, T.J., Higgins, D.G., 2007. ClustalW and ClustalX version 2. Bioinformatics 23, 2947-2948.

584 Laskowski, R.A., MacArthur, M.W., Moss, D.S., Thornton, J.M., 1993. PROCHECK: a program to check the stereochemical quality of protein structures. J. Appl. Crystal. 26, 283-291.

586 Nahoum, V., Farisei, F., Le-Berre-Anton, V., Egloff, M.P., Rouge, P., Poerio, F., Payan, F., 1999. A plant-seed inhibitor of two classes of α-amylases: X-ray analysis of *Tenebrio molitor* larvae α-

588 amylase in complex with the bean *Phaseolus vulgaris* inhibitor. Acta Crystallogr. D55, 360-362.

Nahoum, V., Roux G., Anton V., Rouge, P., Puigserver, H., Bischoff, H., Henrissat, B., Payan, F.,

590 2000. Crystal structures of human pancreatic α-amylase in complex with carbohydrate and proteinaceous inhibitors. Biochem. J. 346, 201-208.

592 Oda Y., Matsunaga T., Fukuyama K., Miyazaki T., Morimoto, T., 1997. Tertiary and quaternary structures of 0.19 α-amylase inhibitor from wheat kernel determined by X-ray analysis at 2.06 Å
594 resolution. Biochemistry 36, 13503-13511.

Payan, F., 2004. Structural basis for the inhibition of mammalian and insect α-amylases by plant
596 protein inhibitors. BBA 1696, 171-180.

Peitsch, M.C., 1995. Protein modeling by E-mail. Bio/Technology, 13, 658-660.

598 Pettersen, E.F., Goddard, T.D., Huang, C.C., Couch, G.S., Greenblatt, D.M., Meng, E C,. Ferrin, T.E., 2004. UCSF Chimera - A visualization system for exploratory research and analysis. J.
600 Comput. Chem. 25, 1605-12, (http://www.cgl.ucsf.edu/chimera).

Pieper, U., Webb, B.M., Barkan, D.T., Schneidman-Duhovny, D., Schlessinger, A., Braberg, H.,
602 Yang, Z., Meng, E.C., Pettersen, E.F., Huang, C.C., Datta, R.S., Sampathkumar, P., Madhusudhan, M.S., Sjölander, K., Ferrin, T.E., Burley, S.K., Sali, A., 2009. MODBASE, a database of annotated
604 comparative protein structure models and associated resources. Nucleic Acids Res. 37, D347-D354.

Salcedo, G., Sánchez-Monge, R., García-Casado, G., Amentia, A., Gomez, L., Barber, D., 2004.
606 The cereal α-amylase/trypsin inhibitor family associated with bakers' asthma and food allergy, in: Mills, E.N.C., Shewry, P.R. (Eds.), Plant Food Allergens, Blackwell Publishing Company, Oxford,
608 pp. 70-86.

Šali, A., Blundell, T.L., 1993. Comparative protein modelling by satisfaction of spatial restraints. J.
610 Mol. Biol. 234, 779-815.

Sánchez-Monge, R., Gomez, L., Barber, D., Lopez-Otin, C., Armentia, A., Salcedo, G., 1992.
612 Wheat and barley allergens associated with baker's asthma. Biochem. J. 281, 401-405.

Sánchez-Monge, R., Gomez, L., García-Olmedo, F., Salcedo, G., 1989. New dimeric inhibitor of
614 heterologous α-amylases encoded by a duplicated gene in the short arm of chromosome 3B of wheat (*Triticum aestivum* L.). Eur. J. Biochem. 183, 37-40.

616 Sánchez-Monge, R., Gomez, L., García-Olmedo, F., Salcedo, G.A., 1986. Tetrameric inhibitor of insect amylase from barley. FEBS Letters 207, 105-107.

618 Shevchenko, A., Wilm, M., Vorm, O., Mann, M., 1996. Mass spectrometric sequencing of proteins from silver-stained polyacrylamide gels. Anal. Chem. 68, 850-858.

620 Silano, V., Furia, M., Gianfreda, L., Macri, A., Palescandolo, R., Rab, A., Scardi, V., Stella, E., Valfre, F., 1975. Inhibition of amylases from different origins by albumins from the wheat kernel.

622 BBA 391, 170-178.

Strobl, S., Maskos, K., Wiegand, G., Hubert, R., Gomis-Ruth F.X., Glockshuber, R., 2004. A novel

624 strategy for inhibition of α-amylases: yellow meal worm α-amylase in complex with the *Ragi* bifunctional inhibitor at 2.5 Å resolution. Structure 6, 911-921.

626 Tovchigrecko, A., Vakser, I.A., 2006. GRAMM-X public web server for protein-protein docking. Nucleic Acids Res. 34, W310-314.

628 Zacharius, R.M., Zell, T.E., Morrison, J.H., Woodlock, J.J., 1969. Glycoprotein staining following electrophoresis on acrylamide gels. Anal. Biochem. 30, 148-152.

630 Zoccatelli, G., Dalla Pellegrina, C., Mosconi, S., Consolini, M., Veneri, G., Chignola R., Peruffo, A., Rizzi, C., 2007. Full-fledged proteomic analysis of bioactive wheat amylase inhibitors by a 3-D

632 analytical technique: identification of a new heterodimeric aggregation states. Electrophoresis 28, 460-466.

634

Figure(1)
Click here to download high resolution image

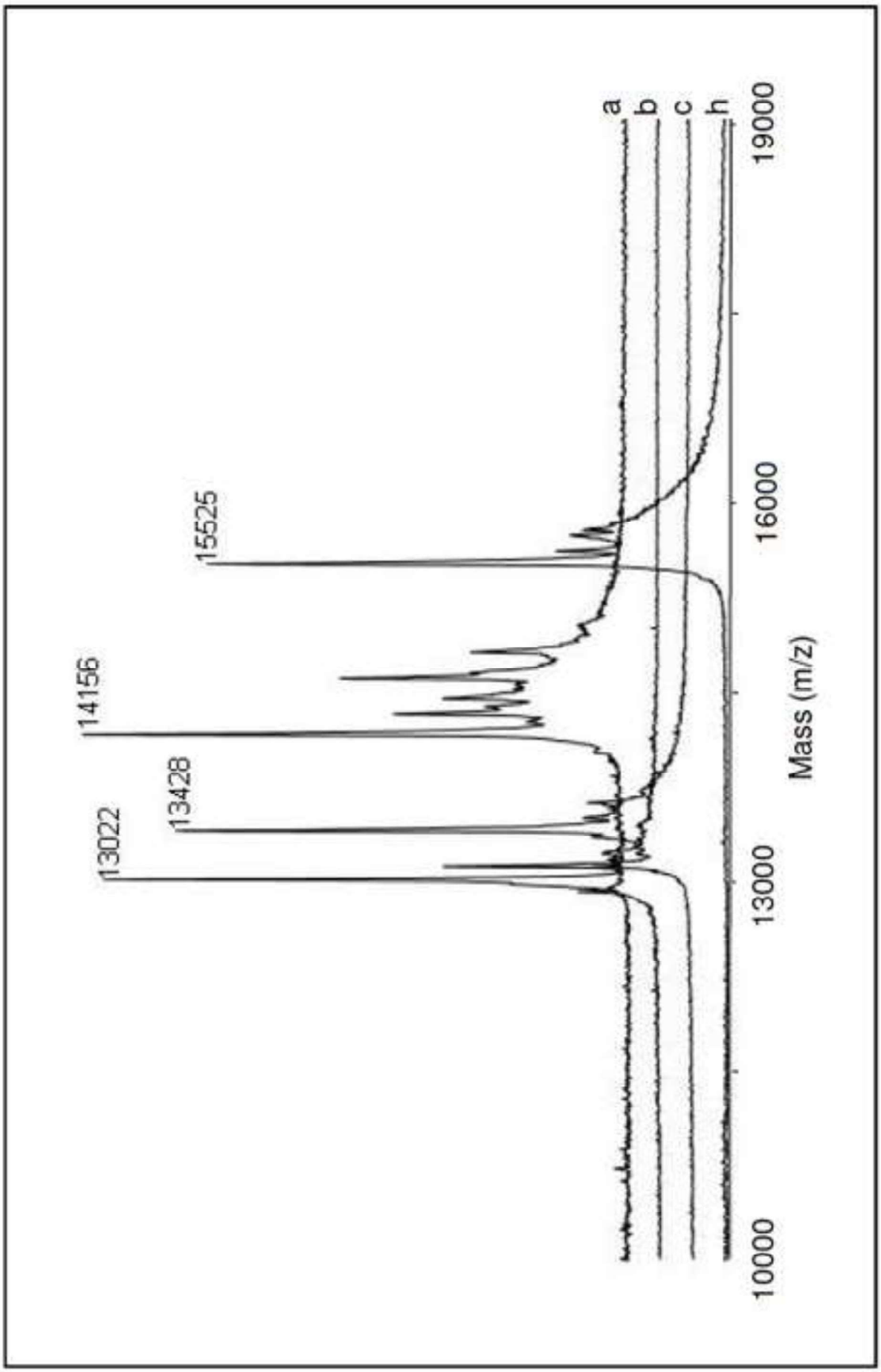

Figure(2)
Click here to download high resolution image

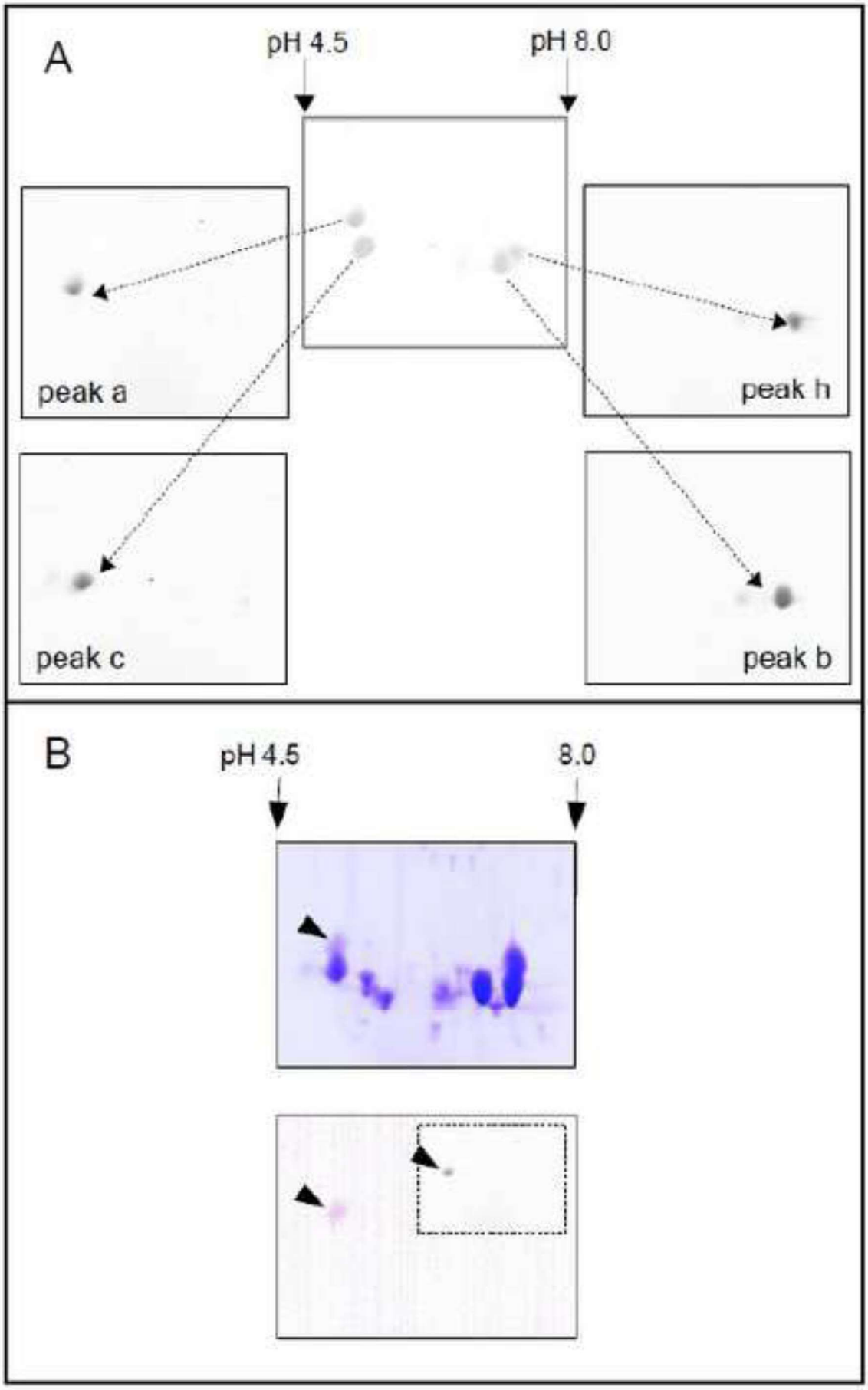

Figure(3)

Click here to download high resolution image

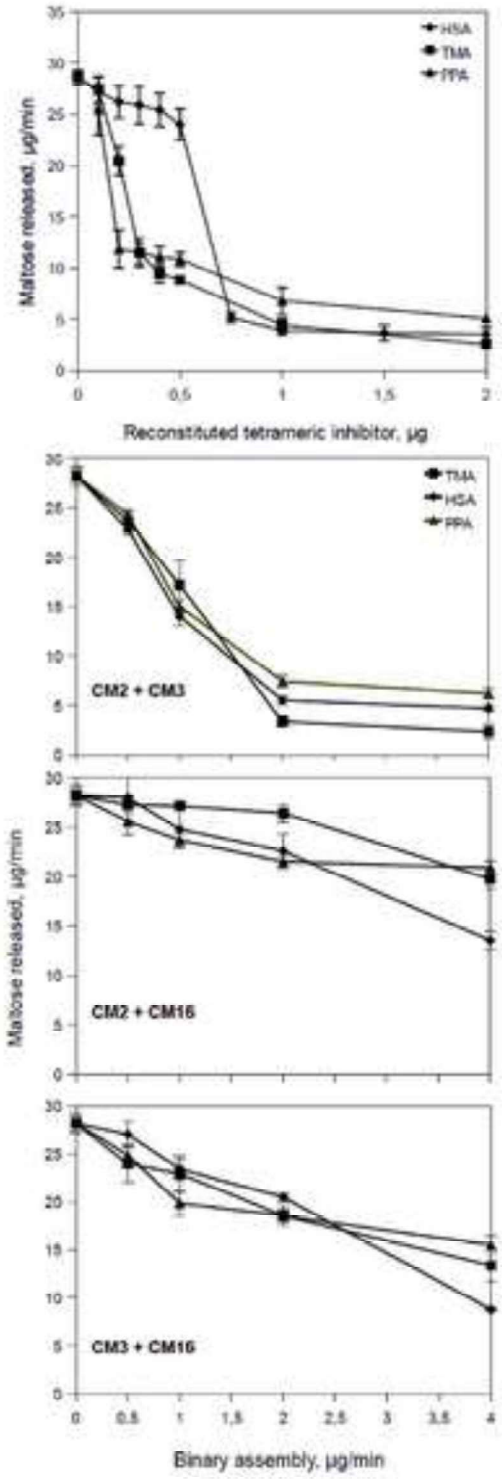

Figure(4)
Click here to download high resolution image

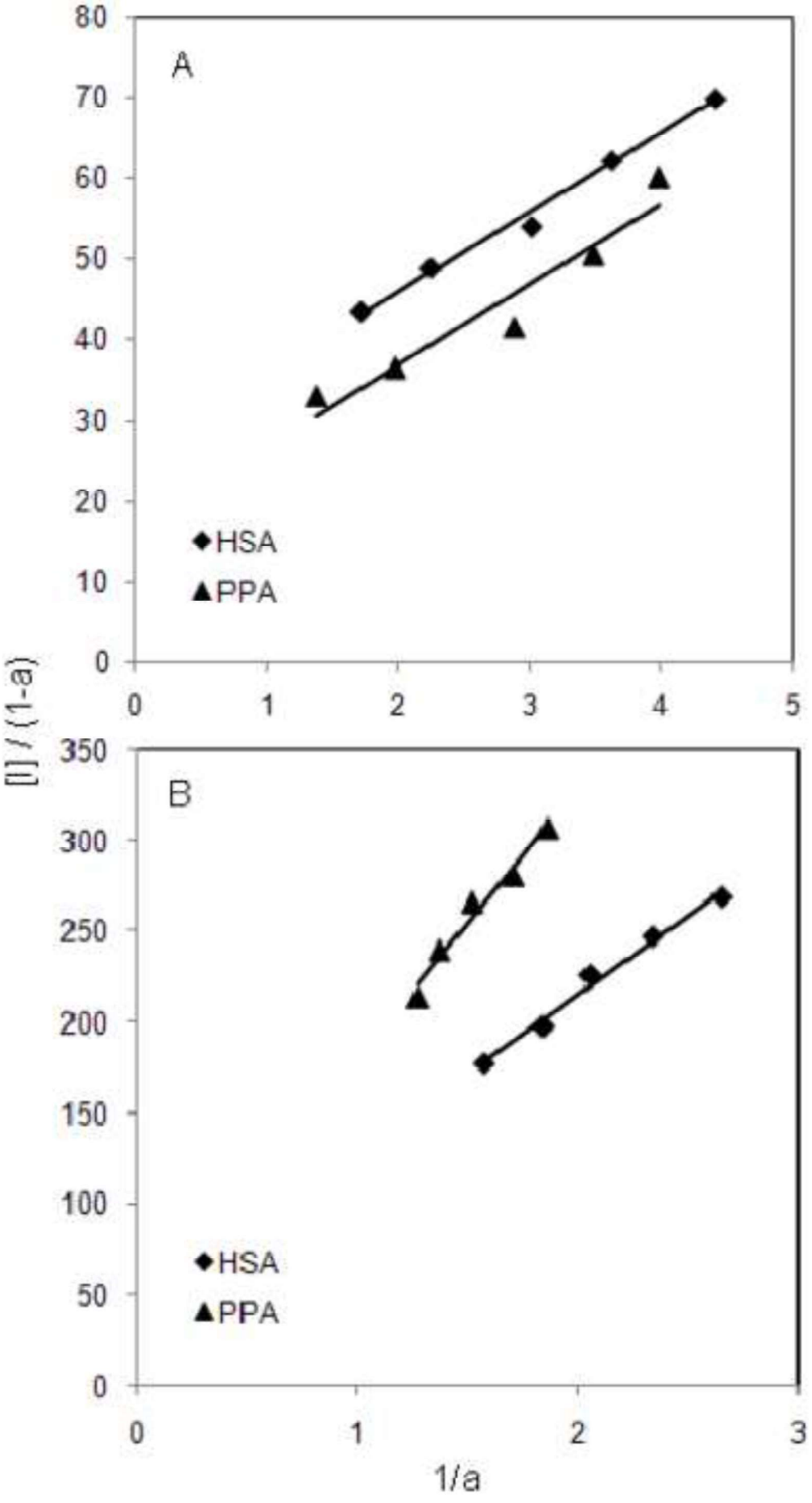

Figure(5)
Click here to download high resolution image

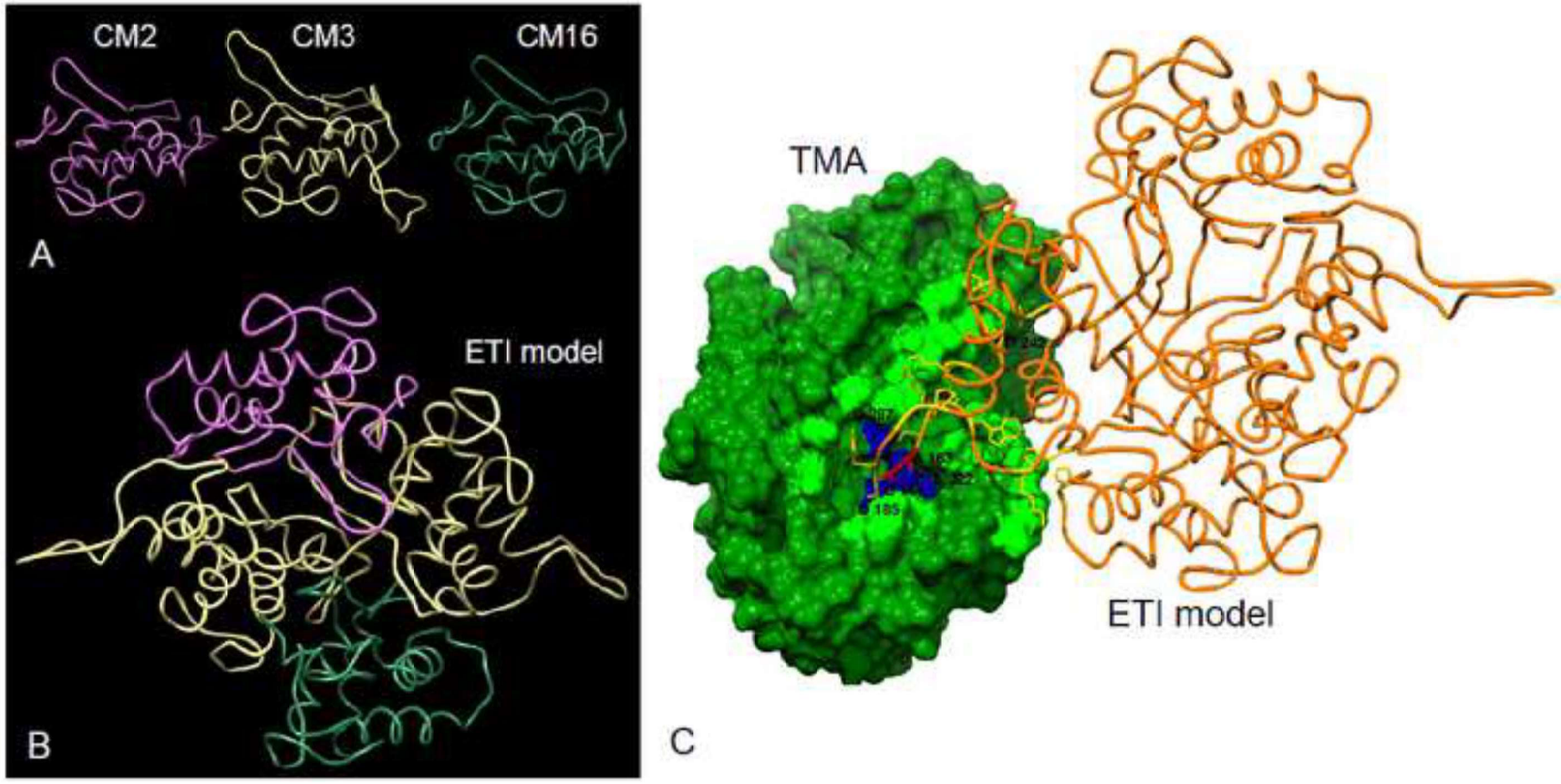

Table(I)

Click here to download Table(s): Table I.doc

CM16

Fragment	Position	MH^+ Monoisotopic	MALDI MS Measured MH^+	ESI MS Measured MH^+	Sequence
T1	1-21	2476.2	2476.2	2476.5	IGNEDCTPWMSTLITPLPSCR
T1'	4-21	2192.0	2191.9	2192.3	EDCTPWMSTLITPLPSCR
T2	22-30	1182.6	1182.6	1182.5	DYVEQQACR
T3	31-41	1175.6	1175.6	1175.2	IETPGSPYLAK
T4	42-56	1903.9	1903.8	1903.3	QQCCGELANIPQQCR
T5	57-61	661.4			CQALR
T6	62-67	742.4	742.4	742.4	YFMGPK
T7	68-83	1813.9	1813.8	1813.9	SRPDQSGLMELPGCPR
T8	84-91	1023.5	1023.5	1023.5	EVQMDFVR
T9	92-119	3312.5	3312.8	3312.9	ILVTPGYCNLTTVHNTPYCLAMEESQWS

CM3

Fragment	Position	MH^+ Monoisotopic	MALDI MS Measured MH^+	ESI MS Measured MH^+	Sequence
T1	1-11	1150.7	1150.6	1150.8	SGSCVPGVAFR
T2	12-19	1024.6	1024.5	1024.6	TNLLPHCR
T3	20-35	1815.9	1815.7	1816.0	DYVLQQTCGTFTPGSK
T4	36-55	2239.1	2239.3	2239.1	LPEWMTSASIYSPGKPYLAK
T5	56-70	2000.2	2000.0	2000.1	LYCCQELAEISQQCR
T6	71-75	662.4			CEALR
T7	76-90	1698.9	1698.9	1699.0	YFIALPVPSQPVDPR
T8	91-107	1741.9	1741.8	1741.8	SGNVGESGLIDLPGCPR
T9	18-115	1110.5	1110.5	1110.5	EMQWDFVR
T10	116-132	1890.1	1890.1	1890.2	LLVAPGQCNLATIHNVR
T11	133-143	1389.8			YCPAVEQPLWI
T11'	133-141	1090.6		1090.3	YCPAVEQPL

CM2

Fragment	Position	MH^+ Monoisotopic	MALDI MS Measured MH^+	ESI MS Measured MH^+	Sequence
T1	1-20	2254.2	2254.0	2254.7	TGPYCYPGMGLPSNPLEGCR
T2	21-46	2717.14	2717.3	2717.3	E YVAQQTCGVGIVGSPVSTEPGNTPR
T3	47-48	290.1			DR
T4	49-51	495.4			CCK
T5	52-61	1292.7	1292.5	1292.8	ELYDASQHCR
T4+T5	49-61	1769.0	1769.7	1769.2	CCKELYDASQHCR
T6	62-66	648.4			CEAVR
T7	67-71	655.4		655.6	YFIGR
T8	72-81	1017.5			TSDPNSGVLK
T9	82-88	828.5			DLPGCPR
T8+T9	72-88	1827.0	1826.9	1827.1	TSDPNSGVLKDLPGCPR
T10	89-92	529.3			EPQR
T8+T9+T10	72-92	2337.3	2337.1	2337.3	TSDPNSGVLKDLPGCPREPQR
T9+T10	82-92	1338.8	1338.6	1338.8	DLPGCPREPQR
T11	93-96	480.2			DFAK

T10+T11	82-96	1799.9	1799.8	1800.0	DLPGCPREPQRDFAK
T12	97-120	2738.5	2738.4	2738.8	VLVTPGHCNVMTVHNTPYCLGLDI

Table I. Fragment nomenclature, position, calculated monoisotopic and experimentally measured MH^+ and sequence of tryptic fragments of the CM16, CM2 and CM3 subunits.